

## Structural Changes of Microbial Transglutaminase during Thermal and High-Pressure Treatment

ORQUÍDEA MENÉNDEZ,<sup>†</sup> HARSHADRAI RAWEL,<sup>‡</sup> UWE SCHWARZENBOLZ,<sup>†</sup> AND  
THOMAS HENLE<sup>\*,†</sup>

Institute of Food Chemistry, Technische Universität Dresden, D-01062 Dresden Germany and Institute  
of Nutritional Science, University of Potsdam, D-14558 Nuthetal, Germany

The activity of microbial transglutaminase (MTG) and the corresponding secondary structure, measured by circular dichroism (CD), was analyzed before and after treatment at different temperatures (40 and 80 °C) and pressures (0.1, 200, 400, 600 MPa). Irreversible enzyme inactivation was achieved after 2 min at 80 °C and 0.1 MPa. Enzyme inactivation at 0.1, 200, 400, and 600 MPa and 40 °C followed first-order kinetics. The enzyme showed residual activity of 50% after 12 min at 600 MPa and 40 °C. Mobility of aromatic side chains of the enzyme molecule was observed in all temperature- and/or pressure-treated samples; however, high-pressure treatment at 600 MPa induced a loss of tertiary structure and a significant decrease in the  $\alpha$ -helix content. The relative content of  $\beta$ -strand substructures was significantly increased after 30 min at 600 MPa and 40 °C or 2 min at 0.1 MPa and 80 °C. We conclude that the active center of MTG, which is located in an expanded  $\beta$ -strand domain, is resistant to high hydrostatic pressure and pressure-induced inactivation is caused by destruction of  $\alpha$ -helix elements with a corresponding influence on the enzyme stability in solution.

**KEYWORDS:** High hydrostatic pressure; secondary structure; tertiary structure, microbial transglutaminase, protein denaturation, circular dichroism

### INTRODUCTION

In recent years, food and drink manufacturers have applied high-pressure processes in order to satisfy consumer's demand for additive-free foods and products with natural, unchanged sensory attributes. In this technology, destruction of vegetative microorganisms in the food is achieved with minimal heating, leading to maximum conservation of vitamins, natural colors, and flavors and thus offering a possibility to produce high-quality food. Some effects of this technology are changes in functional properties of proteins such as emulsifying capacity, gelling, foaming, activation or inactivation of enzymes, and unfolding of their secondary, tertiary, and quaternary structures. Generally speaking, the dissociation of oligomeric proteins is favored at moderate pressure below 150 MPa, whereas treatment at pressures higher than 150–200 MPa may induce unfolding of proteins and reassociation of subunits from dissociated oligomers. At 700 MPa irreversible changes of the secondary structure are observable, whereas even at 1000 MPa covalent bonds of the primary structure are not affected (1–4). The enzyme transglutaminase (protein-glutamine  $\gamma$ -glutamyltransferase, EC.2.3.2.13) catalyzes acyl transfer reactions between the  $\gamma$ -carboxamide group of peptide-bound glutamyl residue and a variety of primary amines (5). Since a microbial

transglutaminase (MTG) is commercially available from fermentation processes, the enzyme has been approved for wide use in the food industry as a processing aid to improve the quality of different food products (6). Previous studies in our laboratories have shown that MTG is remarkably stable under high-pressure treatment, thus enabling the simultaneous application of MTG and high-pressure processing (7, 8). The use of MTG under high hydrostatic pressure offers the possibility of directly affecting the functional properties of proteins which cannot be affected by MTG at atmospheric pressure and therefore reveals new technological possibilities in food production (9). The objective of this work was to study the conformational changes of soluble MTG after high thermal and hydrostatic pressure treatment in relation to enzymatic activity. Secondary and tertiary structure was analyzed by circular dichroism spectroscopy in the near- and far-ultraviolet range. Insoluble protein was analyzed by SDS–PAGE electrophoresis and amino acid analysis.

### MATERIALS AND METHODS

**Materials.** Microbial Transglutaminase Active MP isolated from *Streptococcus mobaraense* was from Ajinomoto Co. Inc. (Hamburg, Germany). This commercial preparation contains 90% lactose, 9% maltodextrin, and 1% protein (w/w) according to the manufacturer's information. N $\epsilon$ -( $\gamma$ -glutamyl)-L-lysine, N $\alpha$ -CBZ-glutamylglycine, L-glutamic acid  $\gamma$ -monohydroxamate, and glutathione in the reduced form were purchased from Sigma (Steinheim, Germany). Ferric chloride was

\* To whom correspondence should be addressed. E-mail: Thomas.Henle@chemie.tu-dresden.de.

<sup>†</sup> Technische Universität Dresden.

<sup>‡</sup> University of Potsdam.

purchased from Grüssing (Filsim, Germany) and tris(hydroxymethyl)-aminomethane from Merck (Darmstadt, Germany).

**Sample Preparation for High-Pressure Treatment.** A solution of 0.029 mg/mL MTG in 0.2 M tris-acetate buffer pH 6.0 was used for the kinetic studies, whereas a solution of 0.29 mg/mL MTG in the same buffer was used for CD measurements.

**High-Pressure and Thermal Treatment of Solutions of MTG.** Solutions of MTG, dissolved in 0.2 M tris-acetate buffer, pH 6.0 (5 mL), were poured in polypropylene tubes and placed in the preheated pressure vessels of the hydrostatic pressure unit. The concentration of MTG was 0.029 mg/mL for kinetic studies or 0.29 mg/mL for CD measurements. High-pressure levels were generated on a high-pressure plant (Bernd Dieckers GmbH, Willich, Germany) using a water–ethylene-glycol mixture for pressure transduction. The pressure was built up at rate of 300 MPa/min, and the decompression time was less than 30 s. Samples were treated for 10–60 min at 0.1, 200, 400, and 600 MPa and 40 °C. After each treatment the enzyme activity and CD spectra were recorded. Another batch of samples was pretreated in a water bath at 60 and 80 °C for 2, 4, 6, 8, and 10 min before measuring the enzyme activity. From this set the sample treated for 2 min at 80 °C was subjected to CD spectra measurement.

**Determination of Enzyme Activity.** This was performed as described in ref 10. MTG solution (0.5 mL) was added to 1 mL of 0.2 M tris-acetate buffer (pH 6.0, containing 0.1 M hydroxylamine, 10 mM glutathione, 30 mM CBZ-L-glutaminyglycine). After incubation at 37 °C for 10 min, 1.5 mL of ferric chloride–trichloroacetic acid reagent (1 vol 12% HCl, 1 vol 12% trichloroacetic, and 1 vol 5% ferric trichloride solution in 0.1 M HCl) was added and the resulting color was measured at 525 nm using an Ultrospec 1000 spectrophotometer (Pharmacia Biotec, Cambridge, England). One enzyme unit was defined as the amount of enzyme which catalyzes the formation of 0.5  $\mu$ mol of hydroxamate per min in the test.

**Circular Dichroism Measurement.** After high-pressure and thermal treatment, the samples were centrifuged at 1200g for 15 min to separate the irreversibly denatured protein, which was investigated further by electrophoresis and amino acid analysis. Soluble proteins of native and treated MTG samples were centrifuged at 1900g in a vivaspin 15R concentrator assembly having a membrane with a 10 000 MWCO (HY, Viva Science, Hannover, Germany) in order to remove lactose and maltodextrins. Seven washings were made with 10 mL of phosphate buffer 0.1 M pH 7.0 until the Fehling sugar method showed that the samples were free of sugars. Far-UV circular dichroism (CD) of the samples was recorded in the range of 178–260 nm at a protein concentration of 0.2 mg/mL phosphate buffer (0.1 M), using a Jasco J 710 spectropolarimeter (Jasco Labor- und Datentechnik GmbH, Gross-Umstadt, Germany). A cylindrical quartz cell having a 1 mm path length was used for the measurements. The following parameters were used: step resolution, 1 nm; speed, 20 nm/min; bandwidth, 1 nm; response, 4 s; sensitivity, 200 mdeg. Mean ellipticity using a molecular weight of 38 kDa and a number of amino acid of 331 for MTG was calculated from the amino acid sequence of the subunits (SWISS-PROT database, <http://us.expasy.org/>, USA). The far-UV CD spectra were analyzed by curve-fitting software CDPPro using the CONTIN method to obtain the secondary structural contents of the proteins. The estimation was performed using a 48-protein reference set (11).

**Sodium Dodecyl Sulfate–Polyacrylamide Gel Electrophoresis.** Irreversible precipitated protein samples (1 mg) were dissolved in 1 mL of 0.4 M Tris-HCl, pH 8.0 buffer containing 2% SDS. The samples were analyzed using sodium dodecyl sulfate–polyacrylamide gel electrophoresis (SDS–PAGE) in gels consisting of layers with different acrylamide concentrations (5%, 7%, 10%) following the procedure of Lane (12). Gels were run on a standard vertical Hoeffer SE 600 electrophoresis unit (Amersham Biosciences, München, Germany).

**Amino Acid Analysis.** Irreversible precipitated protein samples (10–11 mg) were hydrolyzed in the presence of 10 mL of 6 M HCl acid following the procedure of Henle et al. (13). Conventional amino acids, lysinoalanine (LAL), histidinoalanine (HAL), furosine, and pentosidine were measured using an Alpha Plus amino acid analyzer (LKB, Biochrom, Cambridge, U.K.) with a cation-exchange chromatography column. External calibration, running conditions, and data analyses were performed using procedures described by Henle et al. (13, 14). The

eluting amino acids were first detected using an ultraviolet detector K-2501 (Knauer GmbH, Berlin, Germany) at 280 nm and a fluorescence detector RF-535 (Shimadzu Corporation, Kyoto, Japan) at excitation/emission of 335/385 nm, followed by ninhydrin postcolumn derivatization. Integration of the peaks was evaluated using Eurochrom 2000 chromatography software (Knauer GmbH, Berlin, Germany).

**Thermodynamic Data Analysis.** Kinetic parameters were calculated from experimental data using the following terms: reaction order ( $n$ ), rate constants ( $k$ ), and activation volumes ( $\Delta V^*$ ).

In general, an  $n$ th-order rate equation can be written as

$$dA/dt = -kA^n \quad (1)$$

where  $A$  is the response property,  $k$  the rate constant,  $t$  the treatment time, and  $n$  the reaction order. For a first-order reaction, integration of eq 1 for a decay process at constant pressure and temperature is given by

$$\ln[A/A_0] = -k(t - t_0) \quad (2)$$

Applied to enzymes,  $A_0$  in eq 2 is referring to the activity at  $t = 0$  and  $A$  represents the activity at different time points of physical treatment (temperature or pressure)

The pressure dependence of the rate constant ( $k$ ) at a certain temperature is commonly described by the activation volume  $\Delta V^*$  as given in the Eyring relation

$$\ln[k/k_0] = -\frac{\Delta V^*}{RT}(P - P_0) \quad (3)$$

where  $k_0$  is the rate constant at pressure  $P_0$ ,  $P$  is the value of applied pressure,  $\Delta V^*$  is the activation volume at a certain temperature,  $T$  is the absolute temperature, and  $R$  is the universal gas constant.

**Statistical Analysis.** Experiments were repeated three times and evaluated by their means and standard deviation. A maximum of  $\pm 5\%$  standard deviation from the averaged values was generally tolerated. The averaged values are documented in the respective tables and figures. The data were statistically analyzed by ANOVA and Duncan's multiple range test. Significant differences were defined at  $p < 0.05$ .

## RESULTS AND DISCUSSION

**Thermal and High-Pressure Inactivation.** After thermal treatment, residual MTG activity was 11% after 5 min at 60 °C and complete inactivation was achieved after 2 min at 80 °C. Decrease of activity was irreversible, as for such treated samples no reactivation was observed after incubation at 37 °C for 180 min.

Inactivation due to high hydrostatic pressure was analyzed at 40 °C in a pressure range between atmospheric pressure (0.1 MPa) and 600 MPa. Equations 2 and 3 were linearized using logarithmic data transformation. The response value  $[A/A_0]$  as a function of inactivation time at constant temperature revealed that inactivation of MTG followed a first-order kinetic model (Figure 1). Values for rate constant values ( $k$ ) as calculated from the slope of the regression lines in Figure 1 at 0.1, 200, 400, and 600 MPa were  $0.0047 \pm 0.0006$ ,  $0.0097 \pm 0.0015$ ,  $0.018 \pm 0.0013$ , and  $0.047 \pm 0.0030 \text{ min}^{-1}$ , respectively, and showed that inactivation velocity increased with higher pressure. When the rate constants for enzyme inactivation at 40 °C were plotted as a function of pressure, an inactivation volume of  $-10.1 \pm 1.3 \text{ cm}^3/\text{mol}$  was obtained. These values correspond closely to those reported by Lauber (7), who found a value of  $17.4 \pm 4.0$ . Considering Braun–Le Chatelier's principle,  $\Delta V^* < 0$  favors the denaturation of proteins and acceleration of the enzyme inactivation under pressure (15). The inactivation volume of MTG of  $-10 \text{ cm}^3/\text{mol}$  demonstrated that this enzyme has higher stability compared to phosphatase ( $-58 \text{ cm}^3/\text{mol}$ ),

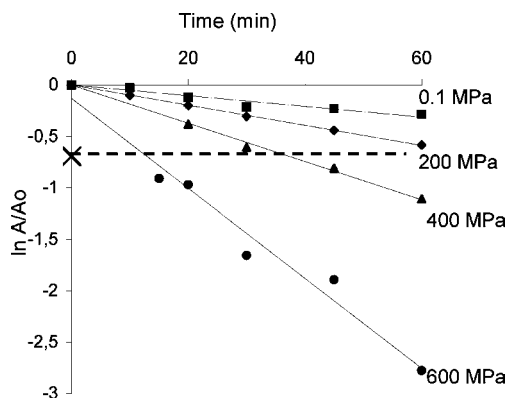


**Figure 1.** Inactivation of MTG by high-pressure treatment at 0.1, 200, 400, and 600 MPa and 40 °C (---) residual activity of 50%

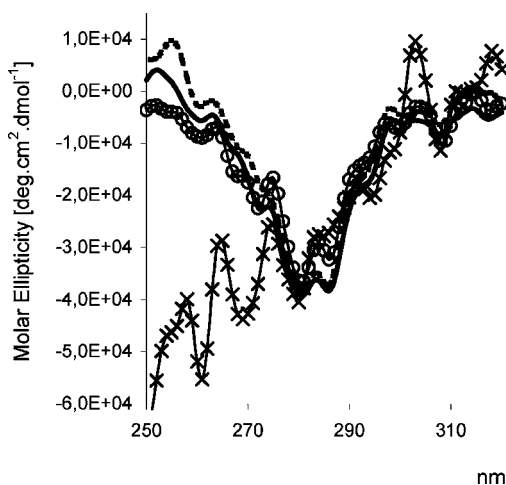


**Figure 2.** Near CD spectra of MTG after thermal and high-pressure treatment: Native MTGase (—), MTGase after 400 MPa, 40 °C, 30 min (···), MTGase after 600 MPa, 40 °C, 60 min (—○—), MTGase after 0.1 MPa, 80 °C, 2 min (—×—).

glutamyltransferase ( $-65 \text{ cm}^3/\text{mol}$ ), or  $\alpha$ -amylase ( $-45 \text{ cm}^3/\text{mol}$ ) at 40 °C (16).

With increasing protein concentration, irreversible precipitation of MTG was observed after 30–60 min treatment at 600 MPa and 40 °C as well as after 2 min at 0.1 MPa and 80 °C. Soluble protein decreased from 0.117 mg/mL in the native sample to 0.091 and 0.066 mg/mL after incubation for 30 and 60 min at 600 MPa and 40 °C, respectively. After treatment for 2 min at 0.1 MPa and 80 °C, only 0.036 mg/mL protein remained in solution. Precipitation of the protein proved that the stability of the native enzyme was a function of high pressure and thermal treatment, revealing a rupture of noncovalent bonds that are responsible stabilizing the conformation of the protein.

#### Analysis of MTG Structure by Circular Dichroism.

Hydrophobic interactions are considered to play an important role in protein folding and protein stabilization. All amino acid residues with aromatic rings in their molecules are hydrophobic; therefore, phenylalanine, tyrosine, and tryptophan are the major constituents of hydrophobic regions (17) and packed in the interior of the protein. For this reason, analysis of CD spectra in the near-ultraviolet wavelength (250–320 nm), which corresponds to the aromatic region, was used to determine the difference between tertiary structure of native and treated MTG (Figure 2). The signal magnitudes and wavelengths of aromatic CD bands cannot be quantitatively calculated. However, the spectrum represents a highly sensitive criterion for the native state of a protein and can be used generally to explain the folded

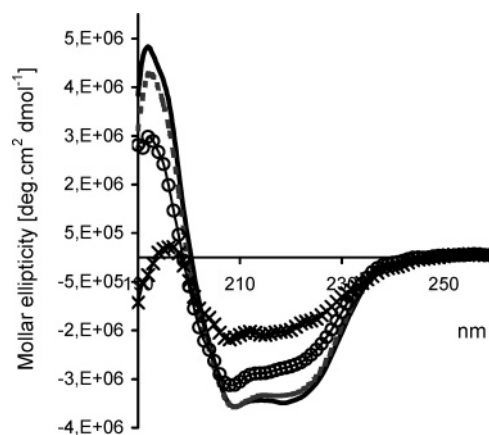


**Figure 3.** Far-UV CD spectra of MTG after thermal and high-pressure treatment. Native MTGase (—), MTGase after 400 MPa, 40 °C, 30 min (···), MTGase after 600 MPa, 40 °C, 60 min (—○—), MTGase after 0.1 MPa, 80 °C, 2 min (—×—).

conformation. CD spectra in the aromatic region are characterized by bands around 252, 256, 262, and 268 nm for phenylalanine, around 275 and 283 nm for tyrosine, and around 290 and 298 nm for tryptophan (18). Spectra of the thermal or high-pressure-treated samples showed different profiles in comparison to the native MTG sample. The intensity of phenylalanine bands increased only in samples treated for 30 min at 0.1, 200, and 400 MPa at 40 °C, but the profile of this band was completely absent in the sample treated for 2 min at 0.1 MPa and 80 °C. The intensity of tyrosine bands at about 283 nm increased proportionally with increasing pressure treatment above 400 MPa at 40 °C for 30 min, and the highest peak was achieved in sample treated at 0.1 MPa and 80 °C for 2 min. Depending on the individual treatment, the intensity of the tryptophan bands (290 and 298 nm) either increased or decreased but did not show a certain tendency. The tertiary structure of the native enzyme was mainly altered at 600 MPa and 40 °C for 60 min, and a short thermal treatment for 2 min at 0.1 MPa and 80 °C was sufficient to achieve a complete unfolded state. Profile bands of phenylalanine and tyrosine were not very distinct, probably because these amino acid residues are located within the hydrophobic MTG region (Figure 2). These hydrophobic regions were not destroyed after the high-pressure treatment but were destroyed after thermal treatment. The band at 283 nm for tyrosine increased distinctly at 0.1 MPa at 80 °C and proportionally with increasing pressure above 400 MPa, which suggests that this amino acid residue is more exposed to the tris-acetate buffer in comparison with phenylalanine and tryptophan residues. The former phenomenon can be explained by the fact that high-pressure and high-thermal treatment changes the polar hydroxyl group of tyrosine from undissociated state at neutral pH and standard conditions to a dissociated state favoring its hydrophilicity (17). Intensity variation of these amino acids was associated with mobility of their aromatic side chains and exposure of their hydrophobic group to the tris-acetate buffer, leading to loss of the MTG tertiary structure and its instability in solution.

Spectra in the far-ultraviolet wavelength region (190–260 nm), which corresponds to the amide region, were used to characterize the conformation structure of the enzyme (Figure 3). Native MTG showed a typical band of the  $\alpha$ -helix  $n-\pi^*$  band at 222 nm and the  $\pi-\pi^*$  band split in to two transitions, namely, a perpendicular  $\pi-\pi^*$  transition band at 191 nm and a parallel  $\pi-\pi^*$  transition band at 208 nm (18, 19). The negative CD signal at 222 nm primarily corresponds to the backbone



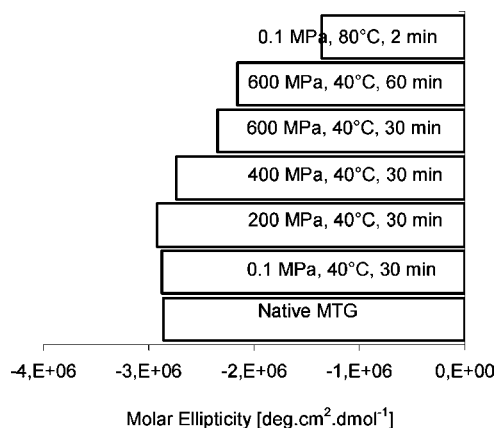


**Figure 4.** CD signals at 222 nm of MTG after thermal and high-pressure treatment.

**Table 1.** Secondary Structure of MTG under High Pressure and Thermal Treatment

| treatment with MTG        | H, <sup>a</sup> % | S, <sup>a</sup> % | Turn, <sup>a</sup> % | Unrd, <sup>a</sup> % | residual activity, % |
|---------------------------|-------------------|-------------------|----------------------|----------------------|----------------------|
| 1. native                 | 24.50             | 23.80             | 21.05                | 30.65                | 100                  |
| 2. 0.1 MPa, 40 °C, 30 min | 23.50             | 23.60             | 21.00                | 31.90                | 85                   |
| 3. 200 MPa, 40 °C, 30 min | 24.20             | 22.90             | 21.00                | 31.90                | 94                   |
| 4. 400 MPa, 40 °C, 30 min | 23.30             | 23.90             | 21.20                | 31.50                | 83                   |
| 5. 600 MPa, 40 °C, 30 min | 19.70             | 25.90             | 20.90                | 33.50                | 55                   |
| 6. 600 MPa, 40 °C, 60 min | 17.20             | 27.50             | 20.55                | 34.75                | 38                   |
| 7. 0.1 MPa, 80 °C, 2 min  | 6.50              | 28.20             | 18.40                | 46.90                | 0                    |

<sup>a</sup> H =  $\alpha$ -helix; S =  $\beta$ -strand; Turn =  $\beta$ -turn; Unrd = unordered.

peptide bond  $n-\pi^*$  transition, which reflects alterations in the secondary structure, especially in the  $\alpha$ -helix content of the enzyme (18, 20). The decreased Cotton effect at 222 nm of MTG reflects alterations in the secondary structure and could suggest that treatment for 30 min at 40 °C above 600 MPa caused drastic changes to the  $\alpha$ -helices of MTG conformation. A short thermal treatment for 2 min at 80 °C was sufficient to achieve maximum loss of the original structure (Figure 4).

Calculation of the relative secondary structure content of the enzyme was performed in the far-UV CD spectra using a CONTIN method (11). The native enzyme consisted of 24.50%  $\alpha$ -helix, 23.80%  $\beta$ -strand, 21.05%  $\beta$ -turn, and 30.65% unordered structure (Table 1). A loss of  $\alpha$ -helix and concomitant increase in unordered structure occurred after high-pressure and thermal treatment. After treatment for 30 min at 400 and 600 MPa, each at 40 °C, the content of  $\alpha$ -helix decreased to 23.30% and 19.70%, respectively. Massive destruction of the  $\alpha$ -helix to a residual amount of 6.5% was achieved after thermal treatment for 2 min at 80 °C. However, after treatment for 30 min at 200 MPa and 40 °C, an increased  $\alpha$ -helix content was observed. Conformational modification of secondary structure was also accompanied by a corresponding loss of enzymatic activity (Table 1). Elevated enzyme activity was recorded with higher contents of  $\alpha$ -helix structure elements. The conformational phenomena described here are in agreement with Tauscher (21), who reported that  $\beta$ -sheet structures are nearly incompressible and more stable against pressure than  $\alpha$ -helix structures. Nosoh (17) reported that hydrophilic residues are found predominantly in  $\alpha$ -helices, which concurs with the tertiary structure of MTG proposed by Kashiwagi et al. (22). The enzyme is arranged in a way that the active site is located between  $\beta$ -strand domains that are surrounded by  $\alpha$ -helices. We hypothesize that pressure-induced degradation of this conformation primarily takes place at the  $\alpha$ -helical areas on the molecule's surface, leading to an alteration of the tertiary structure with subsequent consequences

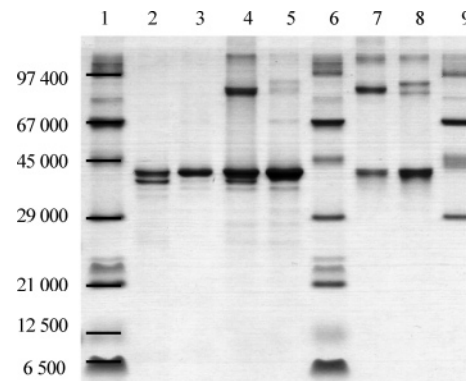


**Figure 5.** SDS-PAGE of MTG after thermal and high-pressure treatment. Lane 1: Molecular mass standard. Lane 2: Nonreduced native MTG. Lane 3: Reduced MTG. Lane 4: Nonreduced MTG; 0.1 MPa/80 °C/2 min. Lane 5: Reduced MTG; 0.1 MPa/80 °C/2 min. Lane 6: Molecular mass standard. Lane 7: Nonreduced MTG; 600 MPa/40 °C/60 min. Lane 8: Reduced MTG; 600 MPa/40 °C/60 min. Lane 9: Molecular mass marker proteins.

on substrate binding. It can be suggested that the enzyme activity at elevated pressures is closely related to the relative stability of the  $\alpha$ -helical regions and the outstanding high-pressure stability of the central  $\beta$ -strand structure.

Irreversible precipitated protein, formed only in samples with a high protein concentration (0.29 mg/mL) after treatment for 60 min at 600 MPa and 40 °C or 2 min at 0.1 MPa and 80 °C, respectively, was analyzed by SDS-PAGE electrophoresis (Figure 5). A representative band of a molecular weight of approximately 40 kDa from reduced native MTG was obtained (Lane 3). Nonreduced sample after thermal treatment showed the representative band of MTG protein and formation of dimers and other compounds with molecular weights between 30 and 90 kDa (Lane 4). Dimers and high molecular weight compounds significantly declined after reduction of the samples but were not completely depolymerized. Nonreduced samples from treatment at high pressure also showed formation of dimers and high molecular weight compounds (Lane 7), and the intensity of these bands after reduction (Lane 8) was higher in comparison to the reduced heat-treated samples. The partial decrease in intensity of dimer bands demonstrated that most of the irreversibly denatured protein after treatment at 0.1 MPa and 80 °C for 2 min and 600 MPa at 40 °C for 60 min was induced by intermolecular disulfide linkages between MTG molecules. Kashiwagi (22) reported that cystein 64 of MTG, which is the catalytic residue in the active center of the enzyme, is located at the bottom of a cleft. Hydropathy analysis of the sequence of the MTG by Kanaji (23) showed that this cystein 64 residue is located in a hydrophobic region situated in the hydrophilic area. High-pressure and thermal treatment of native MTG caused the amino acid residues packed in the interior of the molecule to disperse toward the solvent upon unfolding. Among these amino acid residues, the cystein 64 residue of MTG was exposed more to the tris-acetate buffer and reacted with neighboring cystein residues, leading to formation of disulfides bonds, which caused irreversible protein aggregation.

Incomplete reduction of the bands in lanes 5 and 8 suggested formation of other compounds, which could be preceded by a great variety of reactions such as protein polymerization via isopeptides and Maillard reactions between amino acids residues and lactose, which is a constituent of the commercial MTG preparation. Formation of lysinoalanine and compounds of early and advanced stages of the Maillard reaction have been found

in protein samples treated under high hydrostatic pressure (24, 25). To investigate the noncovalent cross links identified in SDS–PAGE electrophoresis, LAL, HAL, furosine, and pentosidine in the precipitated protein samples were measured after acid hydrolysis via amino acid analysis.

LAL and HAL were not found in native and treated samples (detection limit 2  $\mu\text{g/g}$  protein). Distribution of the products of the early and late stages of Maillard products was variable. Furosine content in the hydrolysates increased from 13.62 to 261.03 and 238.54  $\mu\text{g/g}$  protein in samples treated for 60 min at 600 MPa and 40 °C and 2 min at 0.1 MPa and 80 °C, respectively. The levels of treated samples were not significantly different ( $P > 0.05$ ) and correspond to amounts that can be found in proteins obtained from UHT-treated milk (26). Pentosidine was not detected in the native sample (detection limit 0.02  $\mu\text{g/g}$ ), whereas 13.7 and 6.7  $\mu\text{g/g}$  protein were formed in samples treated for 60 min at 600 MPa and 40 °C or 2 min at 0.1 MPa and 80 °C, respectively. The pentosidine content of the high-pressure sample is significantly different than the heat-treated one and is similar to those of proteins from severely heat-treated foods (i.e., roasted coffee) (14). This is in agreement with the findings of Schwarzenbolz (27) and indicates that the course of the Maillard reaction under high pressure cannot be explained with results known from only thermal treatment. Formation of pentosidine and other currently unknown cross-linking amino acids of the Maillard reaction may contribute to the nonreducible protein oligomerization observed for the samples mentioned above.

In conclusion, the remarkable stability of MTG under high hydrostatic pressure can be explained by the stability of its active site, which is located within an extended  $\beta$ -strand region of the protein. Regions containing  $\beta$ -sheet structures are nearly incompressible and more stable against high hydrostatic pressure than  $\alpha$ -helix structures. Formation of protein cross links, which was observed for selected samples treated for 30 min at 600 MPa and 40 °C or 2 min at atmospheric pressure and 80 °C, was attributed to formation of intermolecular disulfide bonds as well as cross-linking amino acids resulting from the Maillard reaction. To cover the subject of MTG activity fully, further work has to include the possible stabilizing effect of carbohydrates from the commercial enzyme preparation against denaturation. In the end, the remarkable high-pressure stability of MTG makes it a valuable tool for food processing under high-pressure conditions.

#### ABBREVIATIONS USED

MTG, microbial transglutaminase; CD, circular dichroism; SDS–PAGE, sodium dodecyl sulfate–polyacrylamide gel electrophoresis; MWCO, molecular weight cut off; LAL, lysinoalanine; HAL, histidinoalanine; ANOVA, analysis of variance; UHT, ultrahigh temperature.

#### ACKNOWLEDGMENT

We thank Anja Teichmann for technical assistance and Karla Schlosser for amino acids analysis.

#### LITERATURE CITED

- (1) Datta, N.; Deeth, H. High-pressure processing of milk and dairy products. *Aust. J. Dairy Technol.* **1999**, *54*, 41–48.
- (2) Damodaran, S. Food Proteins: An Overview. In *Food Proteins and their Applications*; Damodaran, S., Ed.; Marcel Dekker: New York, 1997; pp 1–7.

- (3) Balny, C.; Masson, P. Effects of high pressure on proteins. *Food Rev. Int.* **1993**, *9*, 611–628.
- (4) Havel, H.; Overview of protein structure and spectroscopic methods. In *Spectroscopic Methods for Determining Protein Structure in Solution*; Havel, H., Ed.; VCH Publishers: New York, 1996; pp 1–4.
- (5) Folk, J.; Chung, S. Molecular and catalytic properties of transglutaminases. *Adv. Enzymol.* **1973**, *38*, 109–191.
- (6) Nielsen, P. Reactions and potential industrial applications of transglutaminase. *Food-Biotechnol.* **1995**, *9*, 119–156.
- (7) Lauber, S.; Noack, I.; Klostermeyer, H.; Henle, T. Stability of microbial transglutaminase to high-pressure treatment. *Eur. Food Res. Technol.* **2001**, *213*, 273–276.
- (8) Lauber, S.; Noack, I.; Klostermeyer, H.; Henle, T. Oligomerization of beta-lactoglobulin by microbial transglutaminase during high-pressure treatment. *Eur. Food Res. Technol.* **2001**, *213*, 246–247.
- (9) Lauber, S.; Krause, I.; Klostermeyer, H.; Henle, T. Microbial transglutaminase crosslinks beta-casein and beta-lactoglobulin to heterologous oligomers under high pressure. *Eur. Food Res. Technol.* **2003**, *216*, 15–17.
- (10) Folk, J.; Cole, P. Mechanism of action of guinea pig liver transglutaminase. I. Purification and properties of the enzyme; identification of a functional cysteine essential for activity. *J. Biol. Chem.* **1966**, *241*, 5518–5525.
- (11) Sreerama, N.; Woody, R. Estimation of protein secondary structure from circular dichroism spectra: comparison of CONTIN, SELCON, and CDSSTR methods with an expanded reference set. *Anal. Biochem.* **2000**, *287*, 252–260.
- (12) Lane, L. A simple method for stabilizing protein-sulfhydryl groups during SDS-gel electrophoresis. *Anal. Biochem.* **1978**, *86*, 655–664.
- (13) Henle, T.; Walter, I.; Krause, H.; Klostermeyer, H. Efficient Determination of Individual Maillard Compounds in Heat-Treated Milk Products by Amino Acid Analysis. *Int. Dairy J.* **1991**, *1*, 125–135.
- (14) Henle, T.; Schwarzenbolz, U.; Klostermeyer, H. Detection and quantification of pentosidine in foods. *Z. Lebensm. Unters. Forsch.* **1997**, *204*, 95–98.
- (15) Jaenicke, R. Biochemical processes under high hydrostatic pressure. Physico-chemical approaches to barosensitivity. *Naturwissenschaften* **1983**, *70*, 332–341.
- (16) Rademacher, B. *Hochdruckbehandlung von Milch. Untersuchung zur Inaktivierung von Mikroorganismen und Enzymen und deren kinetische Beschreibung*; VDI Verlag: Düsseldorf, Germany, 1999.
- (17) Nosoh, Y.; Sekiguchi, T. *Protein Stability and Stabilization through Protein Engineering*; Ellis Harwood: New York, 1991.
- (18) Mulkerrin, M. Protein structure analysis using circular dichroism. In *Spectroscopic Methods for Determining Protein Structure in Solution*; Havel, H., Ed.; VCH Publishers: New York, 1996; pp 5–27.
- (19) Veneres, A.; Rossi, A.; Matteis, F.; Rosato, N.; Agró, A.; Giampiero, M. Opposite effects of  $\text{Ca}^{2+}$  and GTP binding on tissue transglutaminase tertiary structure. *J. Biol. Chem.* **2000**, *275*, 3915–3921.
- (20) Sun, R.; Grant, T.; Dure, L.; Wicker, L. Secondary structure and stability of Marsh grapefruit thermolabile pectinesterase. *J. Agric. Food. Chem.* **1998**, *46*, 3480–3483.
- (21) Tauscher, B. Pasteurization of food by hydrostatic high pressure: chemical aspects. *Z. Lebensm. Unters. Forsch.* **1995**, *200*, 3–13.
- (22) Kashiwagi, T.; Yokoyama, K.; Ishikawa, K.; Ono, K.; Ejima, D.; Matsui, H.; Suzuki, E. Crystal Structure of Microbial Transglutaminase from *Streptovorticillium mobaraense*. *J. Biol. Chem.* **2002**, *277*, 44252–44260.
- (23) Kanaji, T.; Ozaki, H.; Takao, T.; Kawajiri, H.; Ide, H.; Motoki, M.; Shimonishi, Y. Primary structure of microbial transglutaminase from *Streptovorticillium* sp. strain s-8112. *J. Biol. Chem.* **1993**, *268*, 11565–11572.

- (24) Tamaoka, T.; Itoh, N.; Hayashi, R.; High pressure effect on Maillard reaction. *Agric. Biol. Chem.* **1991**, *55*, 2071–2074.
- (25) Schwarzenbolz, U.; Klostermeyer, H.; Henle, T. Maillard reaction under high hydrostatic pressure: studies on the formation of protein-bound amino acid derivatives. In *The Maillard reaction in food chemistry and medical science: Update for the postgenomic era*; Horiuchi, S., Taniguchi, N., Hayase, F., Kurata, T., Osawa, T., Eds.; Elsevier Science: Amsterdam, The Netherlands, 2002; pp 223–227.
- (26) Henle, T.; Zehetner, G.; Klostermeyer, H. Fast and sensitive determination of furosine. *Z. Lebensm. Unters. Forsch.* **1995**, *200*, 235–237.
- (27) Schwarzenbolz, U.; Klostermeyer, H.; Henle, H. Studies on the formation of protein-bound amino acid derivatives as markers of the Maillard reaction under high hydrostatic pressure. *Czech. J. Food Sci.* **2000**, *18 (Spec Issue)*, 65–66.

---

**Received for review September 16, 2005. Revised manuscript received November 24, 2005. Accepted December 8, 2005. This project was financed by Consejo Nacional de Ciencia y Tecnología (CONACYT), México, and Deutscher Akademischer Austauschdienst (DAAD), Germany.**

JF0522863